AINW OBSIDIAN HYDRATION AGE ESTIMATE ANALYSIS METHODS AND PROCEDURES

Jason A. Cowan
March 28, 2023

Atmospheric water diffuses into volcanic glass or obsidian over time to form a rind or rim that thickens with age. Chronological assessment of obsidian through hydration dating provides a way to date artifacts directly rather than associated deposits, albeit with less accuracy and precision than radiocarbon ages and some other archaeological dating methods. Obsidian hydration age estimate analysis performed by Archaeological Investigations Northwest, Inc. (AINW), uses optical measurements of geochemically sourced obsidian hydration rims in conjunction with high-resolution meteorological data, and temporally sensitive projectile point typologies to estimate the age of obsidian artifacts. This age estimation technique was developed to date obsidian artifacts found in the desert areas of eastern California and Nevada (Halford 2008; Rogers 2007, 2010a, 2012; Rogers and Duke 2014). This method minimizes age calculation error caused by differences in ambient temperature experienced by flaked obsidian surfaces as they naturally hydrate when exposed to air. This method also allows for the creation of hydration rates using artifacts collected from disparate sites, and successfully estimates artifact ages from sites not directly associated with the calculation of the source's hydration rate. While other modern hydration analysis techniques (secondary ion mass spectrometry [SIMS] and infrared photoacoustic spectroscopy [IR-PAS]) can be used to effectively estimate artifact ages (Liritzis and Laskaris 2012, Stevenson et al. 2001), the optical microscopy method does not require expensive or bulky equipment, is relatively fast, and provides archaeologically valid chronological assessments.

EFFECTIVE HYDRATION TEMPERATURE (EHT) CALCULATION

The ambient temperature of an artifact undergoing hydration greatly alters the speed of the hydration process; if artifacts with different ambient temperature histories are compared to one another or are used to create a single hydration rate, the results will be highly variable. To compensate for this variability, the ambient temperature history of an artifact with a measured hydration rim must be calculated, and measured rim values must be transformed to an established rate's temperature constant prior to determining a chronological age.

The ambient temperature experienced by any artifact is constantly changing due to daily and yearly temperature fluctuations. Effective hydration temperature is a proxy measurement defined as a constant temperature that yields the same hydration results as an actual location's fluctuating ambient temperature. EHT values will always be greater than the mean annual temperature at a location due to the effect temperature extremes have on the hydration process. Annual and diurnal temperature fluctuations lead to thermal expansion and compression, which allows for faster penetration into the artifact by atmospheric water than if the temperature were constantly at the mean. The EHT captures the constant temperature needed to achieve the same rate of hydration that fluctuating temperatures would cause.

AINW's obsidian age estimate analysis uses a simplified algebraic equation developed to fit Fourier series temperature variation modeling to determine an artifact's EHT (Rogers 2007, 2010a). This method requires knowledge of the artifact's location where hydration occurred, including its depth below surface and several meteorological values such as mean annual temperature, maximum annual variation in temperature, and maximum diurnal variation in temperature at the artifact's location.

Effective Hydration Temperature Equation (Rogers 2007, 2010a)

$$\text{EHT} = T_a \times (1 - Y \times 3.8 \times 10^{-5}) + .0096 \times Y^{0.95}$$

$Y = V_a{}^2 + V_d{}^2$
$V_a = V_{a0} e^{-0.44z}$
$V_d = V_{d0} e^{-8.5z}$

T_a = Mean annual temperature
V_{a0} = Annual temperature variation at surface
V_{d0} = Mean annual diurnal temperature variation at surface
z = Artifact's depth below surface in meters

To determine these meteorological values, high-resolution raster maps were created using 30-year average temperature data (Normals) from weather stations located throughout Oregon and nearby states (U.S. Department of Commerce, National Oceanic and Atmospheric Administration, National Climatic Data Center [NOAA NCDC] 2016). Data gathered from these stations was measured daily between 1981 and 2010 and includes minimum, average, and maximum temperature readings on monthly and yearly scales.

This data and the location data for of each of these weather stations was entered into Arc-GIS and standardized to values at sea-level by using a temperature lapse rate of 5.0 Kelvin (K) Celsius (C)/1,000 meters (2.74° Fahrenheit [F] or 1.52 K (C)/1,000 feet). This step is performed to account for temperature variability due to differences in elevation on the landscape between the weather stations. Temperature lapse rate has been shown to vary considerably over geographic areas. While the chosen rate is less than the international standard atmosphere (ISA) temperature lapse rate of 6.5 K (C)/1,000 m, the rate of 5.0 K is likely higher than the average terrestrial lapse rate for the area (Minder et al. 2010, Wolfe 1964).

Once all data had been corrected to sea level, Gaussian process regression (Kriging) was performed on the data set to create raster maps of values for all areas between the weather stations (Conolly and Lake 2006). Interpolated raster maps were created of average annual temperature and the average, minimum, and maximum monthly temperatures for January and July. Data in these raster maps was then readjusted for elevation variability using the temperature lapse rate and landscape elevation data taken from available 30-m resolution DEM-raster maps of the interpolated area (Figure 1).

These maps, along with provenience data from the obsidian artifact under investigation, contain all the information needed to calculate an artifact's EHT value. Annual temperature variation is calculated by subtracting the average January temperature map from the average July temperature map. Mean annual diurnal temperature variation is found by determining the monthly diurnal temperature variation for January and July and then averaging these two values. Monthly diurnal temperature variation is determined by subtracting the minimum monthly temperature from the maximum monthly temperature. Because ground cover insulates artifacts from temperature extremes, the artifact's depth below ground surface is necessary to calculate EHT. In instances where the depth of the artifact is known, that value was used for the calculation. If the depth of an artifact is recorded to a specific level of a unit, the average depth of that level is used in the EHT calculation.

Sources of error in determining the EHT include the accuracy of the interpolation of weather station readings, normal fluctuations in the annual average temperature, and long-term climatic variation. By collecting data averaged over the last 30 years, errors in the annual fluctuation of average temperature are minimized. Using modern temperature data as a proxy for modeling the climate over archaeological time spans is another source of error. When the model estimates ages, a second EHT transformation can be implemented to adjust the mean estimated age based on paleo climatic data;

however, it has been found that the difference in uncorrected and corrected ages is minimal during the Holocene and is only needed for ages greater than 13,000 years before present (BP) (Rogers 2015; Viau et al. 2006). These sources of error mean that EHT measurements can be no more accurate than 0.5° to 1.0° C (0.9° to 1.8° F) no matter how rigorous the computation method used in the creation of EHT (Rogers 2007).

SOURCE-SPECIFIC HYDRATION RATE CALCULATIONS

Water diffuses into obsidian, like all glass, at a consistent rate, which can be expressed as time (t) multiplied by a constant (k) equals the square of the hydration rim thickness (r). The constant k is the hydration rate.

Hydration Rate Formula (Friedman and Smith 1960)

$$r^2 = kt$$

Many different methods have been used over the years to calculate k. Many have involved comparing the observed rim thickness to radiocarbon measurements or other independently dateable material found in situ with the obsidian item (Baxter 2008; Minor 1985; O'Neill 2004; Pettigrew and Hodges 1995; Wilson 1994). AINW's obsidian age estimate analysis uses hydration rim values measured on artifacts categorized to temporally sensitive projectile point morphological types (point styles) in order to estimate geochemical source specific hydration rates.

The anhydrous chemistry of obsidian influences the hydration rate; therefore, the AINW age estimation model calculates separate hydration rates for each specific geochemical obsidian source. Restricting the rate calculation to individual obsidian sources also controls for variability in the intrinsic water content observed between obsidian sources. Variability in intrinsic water content within individual obsidian sources is not controlled for by the rate calculation. Proxy values for intrasource intrinsic water content variability are used to determine confidence intervals in individual artifact age estimates.

Because there is wide variability in point style temporal spans, AINW uses a weighted linear least-squares best-fit regression analysis to create source specific hydration rates. This method assigns a weight factor to each point style based on the length of time that artifacts associated with the style appear in the archaeological record (Rogers and Duke 2014). This weight factor is inversely related to the square of the time span of the point style. Point styles found during short time spans receive considerably more weight in the regression analysis than point styles found over longer time spans, but all projectile points have some effect in the final hydration rate.

Weighting Factors Equation (Rogers and Duke 2014)

$$w = 1/d^2$$

d = Timespan of projectile point morphological type

Thirty-three different point styles are used to calculate hydration rates (Table 1). Beginning and ending ages for these point styles were constructed from recent archaeological literature on Great Basin (Aikens et al. 2011; Oetting 1994; Smith et al. 2013), Plateau (Lohse 1985; Pettigrew and Hodges 1995), and Southwest Oregon projectile point chronologies (Nilsson and Kelly 1991; Pettigrew and Lebow 1987).

Arrow-sized points that do not fit into a specific morphological style were considered to have an age span similar to the Rosegate Series. Dart-sized corner-notched points not categorized further were considered to have an age span similar to Elko Series points, and generic dart-sized stemmed points were considered to have a span similar to Great Basin (Western) Stemmed.

TABLE 1

PROJECTILE POINT TYPOLOGICAL AGE ESTIMATES AND WEIGHTING FACTOR

Morphological Types	Beginning Age (years BP)	Ending Age (years BP)	Average Age (years BP)	Timespan (d)	Weight Factor (w)*
Great Basin					
Clovis	13,200	12,800	13,000	400	0.5625
Cottonwood Triangular	1000	200	600	800	0.1406
Desert Side-notched	500	200	350	300	1.0000
Elko Series	4500	1000	2750	3500	0.0073
Gatecliff Series	5000	2700	3850	2300	0.0170
Great Basin (Western) Stemmed	14,500	8200	11,350	6300	0.0023
Humboldt Series	6000	1300	3650	4700	0.0041
Northern Side-notched	7500	4000	5750	3500	0.0073
Rosegate Series	2000	200	1100	1800	0.0278
Willow Leaf/Cascade	10,000	1000	5500	9000	0.0011
Plateau					
Cold Springs Side-notched	7800	3700	5750	4100	0.0054
John Day Series	4500	1400	2950	3100	0.0094
Lanceolate Concave Base	12,400	8300	10,350	4100	0.0054
Madras Series	3000	2000	2500	1000	0.0900
Mahkin Shouldered	9000	3700	6350	5300	0.0032
Miller Island Diamond Stem	2300	100	1200	2200	0.0186
Plateau Corner-notched	2300	100	1200	2200	0.0186
Plateau Side-notched	700	100	400	600	0.2500
Quilomene Bar Basal-notched	3200	900	2050	2300	0.0170
Rabbit Island Stemmed	4500	1400	2950	3100	0.0094
Shaniko Series	5700	900	3300	4800	0.0039
Sherman Pin Stemmed	1400	100	750	1300	0.0533
Willow Leaf/Cascade	9000	3700	6350	5300	0.0032
Willowdale Square Barbed	2300	200	1250	2100	0.0204
Southwest Oregon					
Coquille Series (Narrow Necked)	2200	1600	1900	600	0.2500
Coquille Series (Other)	4450	2200	3325	2250	0.0178
Elk Creek Square Barbed	2200	100	1150	2100	0.0204
Rogue River Series (Corner-Notched)	2200	100	1150	2100	0.0204
Rogue River Series (Other)	1600	100	850	1500	0.0400
Side Notched Corner Based	1600	100	850	1500	0.0400
Willow Leaf (Small)	2200	1600	1900	600	0.2500
Willow Leaf (Medium/Large)	4450	2200	3325	2250	0.0178
Willow Leaf (Extra Large)	8450	4450	6450	4000	0.0056

*Weight factors have been normalized so the point style with the shortest time span has a factor of one. Normalizing the weight variable does not affect the least-squares best fit slope formula (Rogers and Duke 2014).

Projectile points used in the hydration rate equations come from a variety of archaeological investigations conducted throughout Oregon (Bajdek et al. 2016; Cadena 2012; Fagan 1996; Fagan et al. 2016; Moratto et al. 1994; O'Neill 2011; O'Neill et al. 1996; Ozbun and Steuber 2001; Ozbun et al. 1996; Winthrop 1989). Because of the additive nature of the regression analysis, hydration rates are constantly

being refined as additional data points are determined. To control for temperature, all artifacts used in these formulas have had their hydration rim measurements transformed to a proxy EHT of 12° C using the Rim Correction Factor (RCF) Calculation described in the Estimated Age Calculation section of this document. On artifacts where multiple surfaces were analyzed and hydration rim measurements varied widely between the different surfaces, the rim measurement used in the rate calculation was taken from the surface best representing projectile point manufacture. Hydration rim measurements are not included in rate calculations if they appeared to come from an area of the artifact with a post-depositional break.

Source-Specific Hydration Rate Equation (k)

$$k = \frac{1}{\left(\frac{\sum w_i x_i y_i}{\sum w_i {x_i}^2}\right)^2}$$

w_i = Morphological type weight factor for each data point
x_i = Rim value at reference EHT for each data point
y_i = Square root of morphological type average age for each data point

Standard Deviation Equation of the Source-Specific Hydration Rate (σ_k)

$$\sigma_k = 2 * \frac{\sigma_s}{S} * k$$

Equations for calculating variables needed by the Hydration Rate Standard Deviation Equation

$$\sigma_s = \sqrt{\left(\frac{\sum w_i {\delta_i}^2}{(n-1)*\sum w_i {x_i}^2}\right)} \qquad \delta_i = \hat{y}_i - y_i \qquad \hat{y}_i = S x_i \qquad S = \frac{\sum w_i x_i y_i}{\sum w_i {x_i}^2}$$

n = Number of artifacts used to compute mean slope

The standard deviation calculated by these formulas produces the range in error in the least-squares best fit equation (Figure 2). It does not account for the other sources of error that affect the artifact age including rim measurement error, variation in intrinsic water content, and error in the EHT calculation. If a hydration rate is not presented with a standard deviation it is because there is currently only one data point available for that obsidian source.

Hydration rates calculated using these equations should always be presented by stating the source and the reference EHT value (ex. Obsidian Cliffs, 3.74 ± 0.31 microns²/1000 years at EHT=12° C). Calculated rates vary dramatically between the different sources. Currently the slowest rate calculated by AINW with at least five data points is for the Gregory Creek obsidian source at 1.94 microns²/1000 years at EHT=12° C, while the fastest calculated rate is from the Massacre Lake/ Guano Valley obsidian source with a rate of 16.20 microns²/1000 years at EHT=12° C.

ESTIMATED AGE CALCULATION

Rim Correction Factor Calculation

The RCF is a number used to transform rim thickness values measured for the artifact under analysis into the equivalent thickness value at a reference location that experienced a different EHT.

Rim Correction Factor Equation (Rogers 2007, 2010a)

$$RCF = e^{[-0.06(\mathrm{EHT}-EHT_{ref})]}$$
$$R_{ref} = RCF * r$$

EHT = Effective hydration temperature of measured artifact
EHT_{ref} = Effective hydration temperature of reference location
r = Hydration rim thickness measurement
R_{ref} = Equivalent hydration rim thickness value at reference location

The RCF value is dependent on the EHT value of the location of the artifact and the EHT of the reference location. The reference location can be an actual location on the landscape or a proxy location set to a specific EHT. Standardizing all hydration rim thicknesses to a specific EHT is necessary for directly comparing hydration rim thickness values.

Age Estimate Calculation

The estimated age equation requires a source-specific hydration rate calculated to a reference EHT and the hydration rim value of the artifact transformed to the same reference EHT as the source specific hydration rate.

Age Estimate Equation (t)

$$t = \frac{(R_{ref})^2}{k_{ref}}$$

k_{ref} = Source specific hydration rate of reference location

Standard Deviation of Mean Estimated Age Calculation

Estimated dates are calculated using techniques designed to minimize error. However, these ages should be viewed cautiously, since each step in the process introduces compounding errors. The primary sources of error come from optical measurement of the hydration rim, climate modeling that produces the EHT, the variability in intrinsic water content of each artifact, and the hydration rate calculation (Liritzis and Laskaris 2011; Rogers 2010b; Rogers and Duke 2014).

To show the variability in these estimated ages, a standard deviation is produced and given along with the estimated age. This error range estimate uses the four primary sources of uncertainty to produce a standard deviation (Rogers 2010b, Rogers and Duke 2014). Proxy values for the error in climate modeling and the variability in an artifact's intrinsic water content are used for this equation, since the actual values are unknown. AINW's obsidian age estimate analysis uses a proxy value of 1° C for climate error because climate modeling is unlikely to be more accurate than this value (Liritzis and Laskaris 2011; Rogers 2010b). A proxy value of 15% intrinsic water variability is used, as this value has been used in previous studies (Rogers and Duke 2014). However, it is important to note that there may be considerably more variability in this source of uncertainty (Rogers 2008). Other proposed values for intrinsic water variability range from 10% to 50% (Rogers 2010b).

Age Estimate Standard Deviation Equation (Rogers and Duke 2014)

$$\sigma_t = 2 * t * \sqrt{\left[\left(\frac{\sigma_r}{r}\right)^2 + (0.06\sigma_{EHT})^2 + \left(\frac{CV_{ks}}{2}\right)^2 + CV_{ke}{}^2\right]}$$

t = Age estimate
r = Hydration rim measurement
σ_r = Standard deviation of hydration rim measurement
σ_{EHT} = Rate of uncertainty in climate modeling
CV_{ks} = Rate of uncertainty due to intrinsic water
CV_{ke} = Coefficient of variation of the hydration rate ascribed to the source

Estimated ages are published in years BP by adjusting the age calculated by the age estimate equation by the number of years between when the rim was measured and 1950. This step is performed to ensure consistency between reported age estimates and for easy comparison to other standard chronological dating methods such as radiocarbon dating. Estimated age and the standard deviation in estimated age are rounded to the nearest 25-year interval and the published age range is a width of four standard deviations centered on the estimated age. Assuming normal distribution in the causes for error used in the standard deviation calculation, four standard deviations captures a 95% confidence interval for the estimated age, and provides a reasonable bracket for the age range.

REFERENCES

Aikens, C. Melvin, Thomas J. Connolly, and Dennis L. Jenkins
2011 *Oregon Archaeology*. Oregon State University Press, Corvallis.

Bajdek, Brennan P., Eva L. Hulse, Jason A. Cowan, Andrea Blaser, and Terry L. Ozbun
2016 *Archaeological Data Recovery at the Burnett Site (35CL96) for the Lake Oswego – Tigard Water Partnership Project, Lake Oswego, Oregon*. Archaeological Investigations Northwest, Inc. Report No. 3563. Prepared for Integrated Water Solutions, LLC.

Baxter, Paul W.
2008 Natural and Induced Hydration Rates of Obsidian Cliffs Obsidian: A case Study from Cascadia Cave. *Current Archaeological Happenings in Oregon* 33(2):11-16.

Cadena, Guadalupe P.
2012 Hunter-Gatherers, Mobility, and Obsidian Procurement: A View From The Malheur Headwaters, Northeast Oregon. Master's Thesis, University of Texas, San Antonio.

Conolly, James, and Mark Lake
2006 *Geographical Information Systems in Archaeology*. Cambridge Manuals in Archaeology. Cambridge University Press, UK.

Fagan, John L.
1996 Obsidian Hydration Analysis of Clovis and Western Pluvial Lakes Tradition Artifacts from the Dietz Site. Paper presented at the 25th Great Basin Anthropological Conference, Lake Tahoe, California.

Fagan, John L., Nicholas J. Smits, Eva Hulse, Jason A. Cowan, Terry L. Ozbun, Jo Reese, Lucie Tisdale, Sarah L. Dubois, Kristen A. Fuld, Karla Hotze, Ron Adams, Cam Walker, Kelley Prince, Maureen M. Zehendner, Morgan Frazier, and Dave Cox
2016 *Ruby Pipeline Project Archaeological Site Testing and Evaluation and Data Recovery, Oregon Segment: Lake and Klamath Counties.* Archaeological Investigations Northwest, Inc. Report No. 3446. Prepared for Ruby Pipeline, LLC and Kinder Morgan, Inc.

Friedman, Irving, and Robert L. Smith
1960 A New Dating Method Using Obsidian. *American Antiquity* 25:476-493.

Halford, F. Kirk
2008 *The Coleville and Bodie Hills NRCS Soil Inventory, Walker and Bridgeport, California: A Reevaluation of the Bodie Hills Obsidian Source (CA-MNO-4527) and its Spatial and Chronological Use*. Cultural Resources Report CA-170-07-08. U.S. Department of the Interior, Bureau of Land Management, Bishop Field Office, California.

Liritzis, Ioannis, and Nikolaos Laskaris
2011 Fifty Years of Obsidian Hydration Dating in Archaeology. *Journal of Non-Crystalline Solids* 357:2011-2023.
2012 The SIMS-SS Obsidian Hydration Dating Method. In *Obsidian and Ancient Manufactured Glasses,* edited by Ioannis Liritzis and Christopher M. Stevenson, pp. 26-45. University of New Mexico press, Albuquerque.

Lohse, Ernest S.
1985 Rufus Woods Lake Projectile Point Chronology. In *Summary of Results, Chief Joseph Dam Cultural Resources Project, Washington*, edited by Sarah K. Campbell, pp. 317-364. Office of Public Archaeology, Institute for Environmental Studies, University of Washington, Seattle. Prepared for U.S. Army Corps of Engineers, Seattle District, Washington.

Minder, Justin R., Philip W. Mote, and Jessica D. Lundquist
2010 Surface temperature lapse rates over complex terrain: Lessons from the Cascade Mountains. *Journal of Geophysical Research* 115:D14122.

Minor, Rick
1985 Hydration Analysis of Obsidian from the Flanagan Site. In *The Flanagan Site: 6,000 Years of Occupation in the Upper Willamette Valley, Oregon*. Unpublished Ph.D. dissertation of Kathryn Anne Toepel, Department of Anthropology, University of Oregon, Eugene.

Moratto, Michael J., Richard M. Pettigrew, Barry A. Price, Lester A. Ross, and Randall F. Schalk
1994 *Archaeological Investigations PGT-PG&E Pipeline Expansion Project, Idaho, Washington, Oregon and California.* Volume I: Project Overview, Research Design and Archaeological Inventory. Michael J. Moratto, General Editor. INFOTEC Research, Inc. Fresno, and Far Western Anthropological Research Group, Inc., Davis, California. Submitted to Pacific Gas Transmission Company.

Nilsson, Elena, and Michael S. Kelly
1991 *Prehistory of the Upper Rogue River Region: Archaeological Inventory and Evaluation within the Elk Creek Lake and Lost Creek Lake Project Areas, Jackson County, Southwest Orego*n. 2 volumes. Mountain Anthropological Research, Chico, California. Submitted to U. S. Army Corps of Engineers, Portland District, Contract No. DACW57-89-C-0067.

Oetting, Albert C.
1994 Chronology and Time Markers in the Northwestern Great Basin: the Chewaucan Basin Cultural Chronology. In *Archaeological Researches in the Northern Great Basin: Fort Rock Archaeology Since Cressman*, edited by C. Melvin Aikens and Dennis L. Jenkins, pp. 41-62. University of Oregon Anthropological Papers 50, Eugene.

O'Neill, Brian L.
2011 Evaluation of the Neil Creek Site (35JA765), *Jackson County, Oregon*. Oregon State Museum of Anthropology Report 2011-001. Museum of Natural and Cultural History, University of Oregon, Eugene.

O'Neill, Brian L., Thomas J. Connolly, and Dorothy E. Freidel
1996 *Streamside Occupations in the North Umpqua River Drainage Before and After the Eruption of Mount Mazama. A Report on the Archaeological Data Recovery Excavations in the Steamboat Creek to Boulder Flat Section, North Umpqua Highway, Douglas County, Oregon*. Oregon State Museum of Anthropology Report 96-2. State Museum of Anthropology, University of Oregon, Eugene.
2004 *A Holocene Geoarchaeological Record for the Upper Willamette Valley, Oregon: The Long Tom and Chalker Sites*. University of Oregon Anthropological Papers 61. Museum of Natural History and the Department of Anthropology, University of Oregon, Eugene.

Ozbun, Terry L., and Daniel Stueber
2001 Obsidian Clovis Points in Western Oregon. *Current Archaeological Happenings in Oregon* 26(2):21-26.

Ozbun, Terry L., Douglas C. Wilson, Eric E. Forgeng, Julia J. Wilt, and John L. Fagan
1996 *Enhanced Survey, Testing and Evaluation Results for Cultural Resources Found on the Elk Creek Road Improvements Project, Jackson County, Oregon*. Archaeological Investigations Northwest, Inc. Report No. 112. Prepared for David Evans and Associates, Portland, Oregon, and the Federal Highway Administration, Vancouver, Washington.

Pettigrew, Richard M., and Charles M. Hodges
1995 Prehistoric Hunter-Gatherer Land-Use Systems: Pacific Northwest. In *Synthesis of Findings*, edited by Randall F. Schalk, pp. 2-1 - 2-70. Archaeological Investigations PGT-PG&E Pipeline Expansion Project Idaho, Washington, Oregon, and California, vol. IV, Michael J. Moratto, general editor. INFOTEC Research, Inc., Fresno, California, and Far Western Anthropological Research Group, Inc., Davis California. Submitted to Pacific Gas Transmission, San Francisco.

Pettigrew, Richard M., and Clayton G. Lebow
1987 *Data Recovery at Sites 35JA27, 35JA59, and 35JA100, Elk Creek Lake Project, Jackson County, Oregon,* 2 Vols. INFOTEC Research Report No. PNW87-7, Eugene, Oregon. Prepared for U.S. Army Corps of Engineers, Portland District, Contract No. DACW57-86-C-106.

Rogers, Alexander K.
2007 Effective hydration temperature of obsidian: a diffusion theory analysis of time-dependent hydration rates. *Journal of Archaeological Science* 34:656-665.
2008 Obsidian hydration dating: accuracy and resolution limitations imposed by intrinsic water variability. *Journal of Archaeological Sciences* 35:2009-2016.
2010a The Obsidian Hydration Cook Book: Aid for the Mathematically Disinclined. *International Association for Obsidian Studies Bulletin* 43:6-13.
2010b Accuracy of Obsidian Hydration Dating Based on Obsidian-radiocarbon Association and Optical Microscopy. *Journal of Archaeological Sciences* 37:3239-3246.
2012 Temperature Correction for Obsidian Hydration Dating. In *Obsidian and Ancient Manufactured Glasses,* edited by Ioannis Liritzis and Christopher M. Stevenson, pp. 46-55. University of New Mexico press, Albuquerque.
2015 A Method for Correcting OHD Age for Paleo-temperature Variation. *Bulletin of the International Association for Obsidian Studies* 52: 3-20.

Rogers, Alexander K., and Daron Duke
2014 Estimating Obsidian Hydration Rates From Temporally-Sensitive Artifacts: Method and Archaeological Examples. *International Association for Obsidian Studies Bulletin* 51:31-38.

Smith, Geoffrey M., Pat Barker, Eugene M. Hattori, Anan Raymond, and Ted Goebel
2013 Points in Time: Direct Radiocarbon Dates on Great Basin Projectile Points. *American Antiquity* 78(3):580-594.

Stevenson, Christopher M., Ihab M. Abdelrehim, and Steven W. Novak
2001 Infra-red Photoacoustic and Secondary Ion Mass Spectrometry Measurements of Obsidian Hydration Rims. In *Journal of Archaeological Science,* No. 28 (2001), pp. 109-115.

U.S. Department of Commerce, National Oceanic and Atmospheric Administration, National Climatic Data Center (NOAA NCDC)
2016 Data Tools: 1981-2010 Normals, Electronic database, http://www.ncdc.noaa.gov/cdo-web/datatools/normals/, accessed August 8 and September 9, 2016.

Viau, A. E., K. Gajewski, M. C. Sawada, and P. Fines
2006 Millennial-scale temperature variations in North America during the Holocene. *Journal of Geophysical Research* 111:D09102.

Winthrop, Kate
1996 *Excavations at the Colvard Site 35JA222, Jackson County, Oregon*. Bureau of Land Management, Medford, Oregon.

Wilson, Douglas C.
1994 Obsidian Procurement and Use in the Willamette Valley, Oregon. Paper presented at the 47th Annual Northwest Anthropological Conference, Spokane, Washington.

Wolfe, Jack A.
1964 *An Analysis of Present-Day Terrestrial Lapse Rates in the Western Conterminous United States and Their Significance to Paleoaltitudinal Estimates*. U.S. Geological Survey Bulletin 1964, U.S. Department of the Interior.

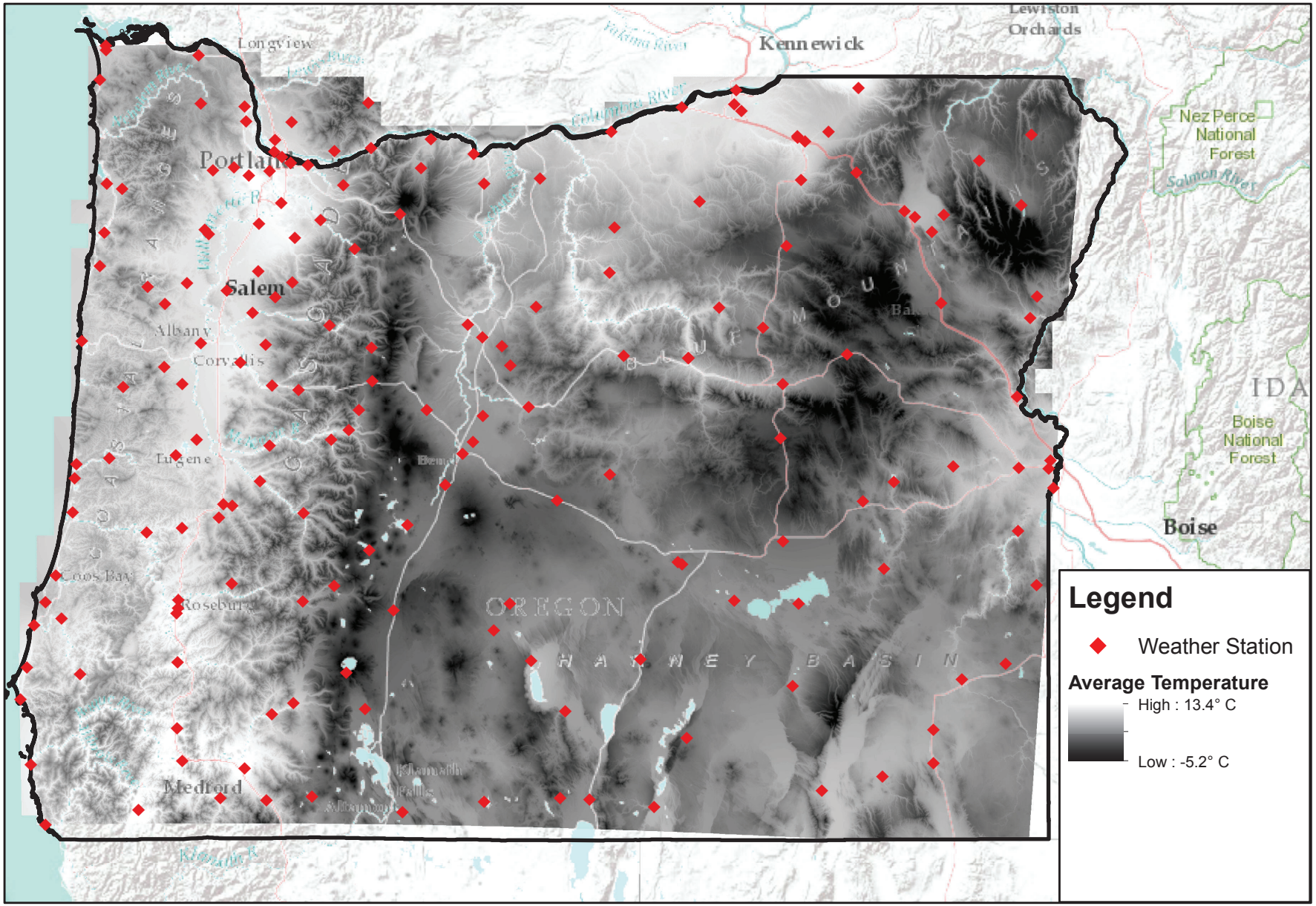

Figure 1. Location of weather stations and interpolated average temperatures used to calculate EHT.

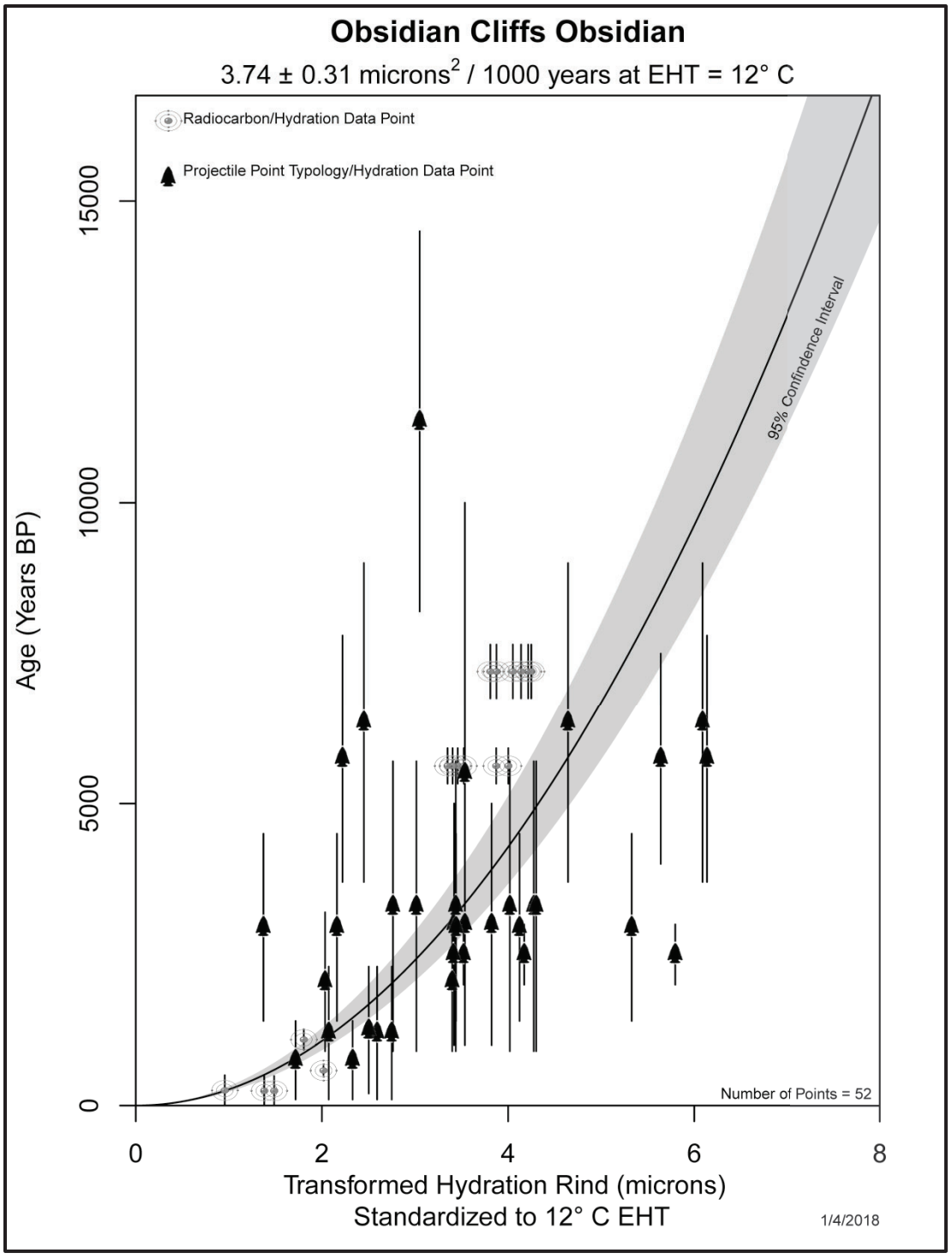

Figure 2. Obsidian Cliffs obsidian hydration rate (exponential curve). The shaded area around the solid curved line indicates 95% confidence in the rate equation. Hydration rim measurements paired with temporally sensitive projectile points are indicated by a projectile point on the graph. Hydration rim measurements paired with a radiocarbon date are indicated by a carbon atom on the graph. The timespan of radiocarbon dates and projectile point styles is shown by the vertical line associated with each data point.